2023 45th Annual International Conference of the IEEE Engineering in Medicine & Biology Society (EMBC) | 979-8-3503-2447-1/23/$31.00 ©2023 IEEE | DOI: 10.1109/EMBC40787.2023.10340450

Optimizing Transcutaneous Oxygen Measurement Sites on Humans

Abigail Leonardi[1*], Ciara Murphy[1*], Sydney Hobson[1*], Vanshika Rohera[1*], Vladimir Vakhter[1*], Burak Kahraman[1], Guixue Bu[2], Foroohar Foroozan[2], Lawrence Rhein[3], and Ulkuhan Guler[1]

***Abstract*— This study utilizes an optical method of transcutaneous oxygen sensing that has the potential to revolutionize at-home care. This technique is based on quenching the luminescence of a platinum porphyrin film. Since oxygen quenches luminescence, its lifetime is further measured to assess the partial pressure of transcutaneous oxygen diffusing through the skin. Unlike conventional transcutaneous oxygen monitors that use electrochemical sensors, the luminescence-based sensor allows the use of dry electrodes that do not require heating and reduce the risk of accidental skin irritations or burns. These properties not only improve patient safety but also allow the creation of miniature wearable transcutaneous oxygen sensors for continuous and accurate remote respiratory monitoring. To this end, it is critical to assess the efficiency of the wearable sensor by determining the optimal location for its placement on the body. Depending on the location on the body, physiological factors such as blood flow rate and skin thickness affect dermal perfusion of transcutaneous oxygen. In this work, four healthy volunteers participated in subject testing. We assessed each participant at the following locations: thumb, top of the wrist, forearm, thigh, and shin. All locations consistently reported accurate and reliable data. Among them, the thumb demonstrated shorter settling times and the most uniform luminescence lifetime values.**

I. Introduction

Respiratory diseases impact millions of people worldwide [1]. In fact, two of the top five leading causes of death are respiratory illnesses: chronic obtrusive pulmonary disease (COPD) and lower respiratory disease [2]. Recently, the coronavirus disease of 2019 (COVID-19) exacerbated these issues contributing to over 6.5 million deaths [1]. The ability to remotely and continuously monitor respiration parameters, including respiration rate and oxygenation parameters such as blood oxygen partial pressure ($\mathrm{PaO_2}$) and blood oxygen saturation ($\mathrm{SaO_2}$), using miniature wearable devices in the early stages of the disease would provide health care professionals with accurate data to create patient-specific treatment plans [3]. Early detection of respiratory diseases would minimize the burden on the health care system [4].

The circulatory system delivers oxygen to body tissues as schematically depicted in Fig. 1. Blood is oxygenated in the lungs and then circulated around the body through arteries. Microcirculation is responsible for oxygen delivery from the red blood cells to the tissues. This delivery of oxygen is administered by the capillaries which are small blood vessels branching off from arteries. The oxygen content in the blood is highest on the arteriole end of the capillary [5]. As the blood flows through the capillaries, oxygen diffuses to the tissues. The partial pressure of transcutaneous oxygen ($\mathrm{PtcO_2}$) measures the oxygen released through the skin, and it is correlated with blood oxygen levels [6].

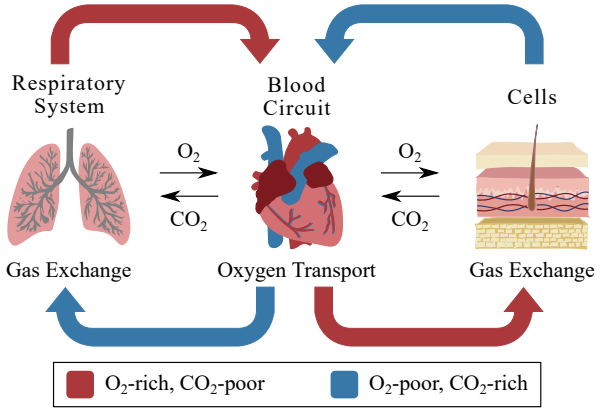

Fig. 1. Oxygenation and circulation of blood in the body.

Monitoring $\mathrm{PtcO_2}$ is a technique that offers several advantages over both arterial blood gas (ABG) monitoring (the current golden standard) and pulse oximetry ($\mathrm{SpO_2}$) [7]. For instance, compared to ABG, transcutaneous devices are noninvasive. Compared to $\mathrm{SpO_2}$, $\mathrm{PtcO_2}$ monitors are more suitable for assessing the $\mathrm{PaO_2}$ [8] due to the direct correlation between these parameters [6]. Large commercial $\mathrm{PtcO_2}$ monitors (such as by Radiometer [9]) already exist. However, these devices are expensive, wired to a wall power outlet, and prohibitively difficult to use outside the clinical settings. Wearable $\mathrm{PtcO_2}$ sensors would allow monitoring of the patient's blood-oxygen status and changes in the arteries, tissues, and cells [10] continuously and remotely, which would improve the quality of the patient's life and provide medical professionals with up-to-date information.

A recent wearable presented in [11], utilizes a luminescent oxygen-sensing film to measure $\mathrm{PtcO_2}$ on the skin surface. The material of the film, platinum porphyrin (Pt-porphyrin), consists of functional groups known as fluorophores whose fluorescence is suppressed in the presence of $\mathrm{O_2}$. When the film is excited with blue light (peak emission wavelength of 450 nm), the fluorophore is excited to a higher energy state. The molecule falls back to a lower energy state and emits a photon of red light (peak emission wavelength of

*These authors contributed equally to this work.

[1]Authors are with Electrical and Computer Engineering Department, Worcester Polytechnic Institute, Worcester, MA 01609, USA (e-mail: {awleonardi, cmurphy5, sahobson, vrohera, vvvakhter, bkahraman, uguler}@wpi.edu).

[2]Authors are with Analog Devices, Inc., Wilmington, MA 01887, USA (e-mail: {guixue.bu, foroohar.foroozan}@analog.com).

[3]Authors are with Department of Pediatrics, UMass Chan Medical School, University of Massachusetts, Worcester, MA 01605, USA (e-mail: {lawrence.rhein}@umassmemorial.org).

This material is based upon work supported in part by the National Science Foundation (NSF) under Grant OAC-2203827 and Analog Devices Inc. through a research gift. Corresponding author: Ulkuhan Guler.

650 nm). If oxygen is present, it will reduce the number of photons emitted. The partial pressure of O_2 around the film is inversely proportional to the intensity and lifetime (τ) of the emitted red light. The lifetime-based method is more reliable since it is less affected by optical path changes [11].

Previous studies have investigated suitable locations for traditional $PtcO_2$ sensors [12]. In this paper, we aim to determine the optimal location on the human body to conduct $PtcO_2$ measurements using the novel $PtcO_2$ sensor, presented in [11]. Identifying suitable locations on the body allows for consistent and accurate $PtcO_2$ readings. This paper is organized as follows. Section II covers our approach, involving a biological rationale for this experiment. Section III details instrumentation, the experimental setup, and data processing using MATLAB. Sections IV and V demonstrate the results and discuss our findings, respectively. Finally, concluding remarks are given in Section VI.

II. Experimental Approach

The $PtcO_2$ is based on the oxygen delivery from the blood to the tissues and oxygen consumption by the tissues [13]. Understanding the physiology behind $PtcO_2$ and the circulatory system is crucial to interpreting sensor measurements, which can vary due to the rate of blood flow, diffusion distance, rate of gas exchange, capillary density, epidermis thickness, and subcutaneous fat thickness. Increased dermal perfusion results in more blood delivering oxygen to the tissues within the body. Blood flow redistribution ensures that no tissues are overperfused at the expense of others [14].

A. Diffusion Distance

A greater diffusion distance results in less oxygen from the capillaries diffusing to the epidermis, therefore reducing $PtcO_2$ [15]. The diffusion distance between the capillaries and the epidermis increases due to subcutaneous fat and epidermal thickness [15].

B. Capillary Density

A study has suggested that $PtcO_2$ depends on the capillary density [15]. Maintaining a highly perfused capillary density will result in smaller diffusion distances from capillary to tissue [14]. The density of capillaries in the skin varies between individuals and differing body locations [16].

III. Implementation and Data Collection

A uniform procedure was utilized in the experimental setup to ensure consistent measurements. The experimental data were post-processed for further analysis.

A. Instrumentation

Our prototype contains four primary blocks, illustrated in Fig. 2: (1) a power management unit (PMU); (2) a sensor head; (3) an analog front end (AFE); and (4) a microcontroller unit (MCU). It is powered through either an external DC power supply or a 3 V lithium coin cell battery [17], [18]. The PMU converts input power to provide separate voltage rails needed to power other sections.

The sensor head consists of a blue light emitting diode (LED) (LXZ1-PR01 by Lumileds) with a peak emission at

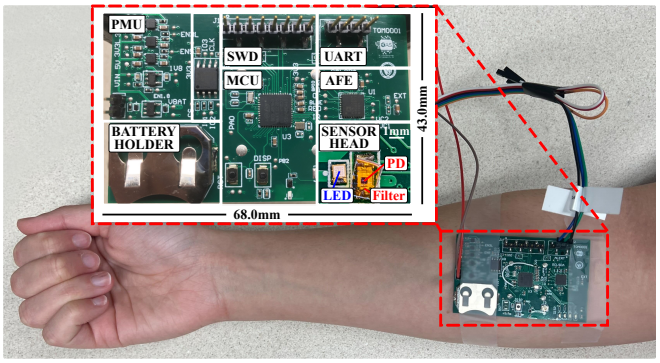

Fig. 2. Experimental setup: sensor layout and placement on the forearm (shown as an inset, the sensor head is located on the board's bottom side).

450 nm and a photodiode (PD) (D019-141- 411-R by Advanced Photonix) sensitive to red light (with a responsivity of 0.05 A/W at the peak wavelength of 600 nm), as shown in Fig. 2. A Pt-porphyrin O_2-sensitive fluorophore die (Red Eye by Ocean Insight) is placed between the skin and the sensor head. The Pt-porphyrin has finite lifetime values, ranging from $\sim$1 μs for high oxygen partial pressures to tens of μs for low oxygen partial pressures [19], [20].

The AFE (ADPD4101 by Analog Devices Inc.) performs the following operations: (1) driving the LED; (2) processing the optical response of the PD to an analog signal; and (3) digitizing this analog signal for storage in its first-in-first-out (FIFO) memory buffer. In addition, the MCU (STM32WB35CC by STMicroelectronics) is employed to: (1) configure the AFE and (2) transmit the digitized optical data to a personal computer (PC). Communication between the MCU and AFE occurs through the Inter-Integrated Circuit (I^2C) bus, whereby the MCU retrieves data from the FIFO of the AFE. Subsequently, the data is transmitted to a PC via a Universal Asynchronous Receiver-Transmitter (UART) interface for τ calculations. More details about the system design can be found in our previous work [11].

Luminescence lifetime is decoupled from the excitation power at low LED currents ($<$ 100 mA), resulting in inaccurate measurement of lifetime [21]. This is because, at lower LED current levels due to insufficient excitation of luminophores molecules, the data becomes noisier, leading to a decrease in the signal-to-noise ratio (SNR) [21]. Thus, a gas sweep experiment was conducted with a sufficiently high LED current of 250 mA in a controlled environment to correlate lifetime values with PO_2 values [11]. The lifetime values showed an expected behavior for PO_2 levels ranging from 0 to 418 mmHg, as shown in Fig. 3a. This provides base values for converting lifetime values into PO_2 levels.

B. Measurement Protocol

A uniform procedure was followed for each test. Before placing the sensor on the body, an isopropyl alcohol swab was used to clean the skin. After allowing the area to dry, the sensor was turned on to collect data measuring ambient air before placing it on the respective body part. Ambient air measurements enable accurate post-processing of the data as it serves as a reference to relate the initial data point to the

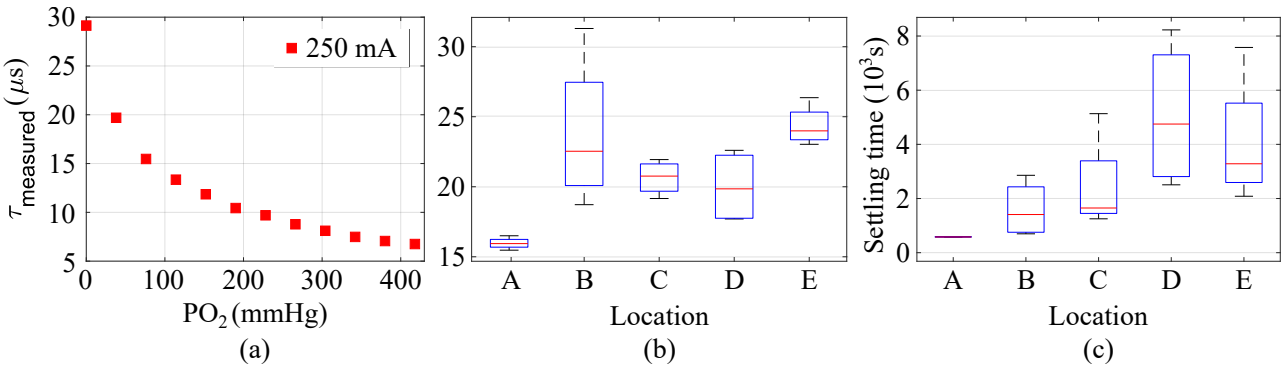

Fig. 3. (a) Sensing film's response to linear PO_2 increase (0-418 mmHg) in a gas experiment using 250 mA LED current [11]. Distribution of experimental data among locations for (b) lifetime value and (c) settling time (locations are denoted as: A - thumb, B - wrist, C - forearm, D - thigh, and E - shin).

atmospheric air pressure. To ensure a stable measurement despite pressure changes, the sensor was affixed to the skin using tubular elastic gauze. The test duration varied depending on each person and location.

The Institutional Review Board of Worcester Polytechnic Institute approved the study protocol (IRB-22-0682). Verbal consent was obtained from all human research participants. The research was performed in accordance with the Declaration of Helsinki [22].

C. Data Collection

We utilized a MATLAB script to process the data received via UART. To get the lifetime information from the received data, we applied an exponential regression using the *fitnlm()* function [11]. At the end of each experiment, we calculated the lifetime value and the settling time of lifetime values (the time required for the oxygen present in the sensing film to stabilize with the oxygen diffusing through the skin [23]). The settling time was identified as the point when all succeeding lifetime values were within 5% of that determined point. The settled τ value from each measurement can be used to interpret PO_2 reading with a conversion rate extracted from the graph in Fig. 3a.

IV. Results and Findings

The lifetime values of various body locations including thumb, forearm, wrist, shin, and thigh were measured on four different test subjects, and their distribution of settling times and lifetime values are depicted in Figs. 3b and 3c. The settling time and τ value of each body location varied across the test subjects, as articulated in Section II and presented in Table I. Certain locations, like the thigh and wrist, showed significantly more variation across test subjects compared to the thumb. The thumb showed the lowest variability in both settling time and value. In comparison, the thigh resulted in the largest variation of settling time 2,500–8,200 s, and the wrist had the most variation in τ values 19–31 μs. Out of five measurement locations the thumb reached its settling point the fastest, reporting an average of 583 s and a standard deviation of 10.69 s. The thumb showed the smallest variation in settling time ranging from 574–598 s, as well as the least variation in lifetime value from 14.10–16.50 μs. The average value for the lifetime value of the thumb was

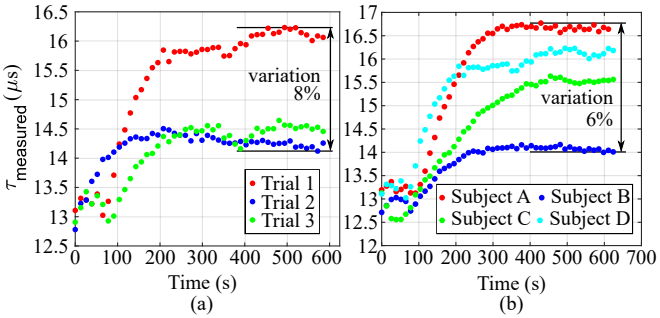

Fig. 4. Lifetime value over time for (a) the thumb of Subject D on three separate days and (b) the thumb of four human subjects.

15.51 μs. There was approximately a 6% difference between the highest and lowest lifetime values, lower than Food and Drug Administration's (FDA) allowable error numbers [24].

In addition, we evaluated the reproducibility of the experiment by collecting three data sets for one body location. The testing took place with uniform conditions as mentioned in Section III. These conditions also include testing on sequential days at the same time each day with no eating prior to the trials. Fig. 4a compares the stabilized lifetime values for one human subject for three days. The first trial reported a setting time of 598 s with a τ value of 15.98 μs. The second trial reported a settling time of 607 s with a τ value of 14.3 μs. The third trial reported a settling time of 621 s with a τ value of 14.4 μs. The results showed an 8% variation when measuring the difference between the maximum and minimum lifetime values. This variation may be explained by the factors, such as physical activity, sleep quality and duration, and food intake, but more investigation is needed to confirm their effect on oxygen levels.

V. Discussion

To determine the optimal location for measuring $PtcO_2$, we used parameters such as settling time, consistency, and variation in lifetime measurements. The data collected from the four subjects represented in Figs. 3b, c, and 4b demonstrate that the sensor is capable of accurately measuring the lifetime value for a variety of different body locations. Moreover, Fig. 4a demonstrates the sensor's ability to reproduce data. Based on the results from the four subjects, the thumb reported the shortest settling time and smallest variation in lifetime value. Determining the optimal location will vary according to the application of the sensor as key criteria will

TABLE I

SETTLING TIMES AND LIFETIME VALUES FOR EACH SUBJECT BY LOCATION

	Subject A		Subject B		Subject C		Subject D	
Testing Locations	Settling time (s)	τ (μs)	Settling time (s)	τ (μs)	Settling time (s)	τ (μs)	Settling time (s)	τ (μs)
Thumb	574	16.50	576	14.10	584	15.47	598	15.98
Wrist	2857	18.72	2006	21.45	812	23.60	697	31.30
Forearm	2650	20.20	1251	21.32	2650	21.94	5133	19.16
Thigh	8226	17.70	3115	21.19	6384	22.6	2506	17.80
Shin	2084	23.03	3100	24.30	3466	26.36	7578	23.68

change. For example, in one use, a smaller settling time may be preferred, or in another application, specific packaging constraints may limit location options.

Although the four subjects exhibited a range of different settling times and lifetime values, slight variations are expected. Each subject differed in fat distribution and muscle density, impacting the diffusion of oxygen at different locations. Data also varied between measurements post-exercise, after food consumption, and sleep quality as these activities impact oxygen uptake in the body. To ensure consistent readings across a diverse range of subjects, a computational model can be trained based on various factors. This computational model will translate the $\mathrm{PtcO_2}$ at any given location on the body and provide blood oxygen levels. This model will ultimately allow for accurate blood oxygen results with varying physiology and underlying diseases. Future work involves designing packaging for the prototype to ensure consistent pressure and sensor contact. Improving the data collection process will account for the biological differences between individuals and adjust measurements accordingly.

VI. CONCLUSION

In this paper, we have presented the use of our novel transcutaneous oxygen monitor to compare readings from various locations on the body of four human subjects. Different body locations yield different values for $\mathrm{PtcO_2}$, indicating biological variability influences $\mathrm{PtcO_2}$. Slight variations in results are expected as the genetics of individuals differ between subjects. Our measurements agree with the previous studies performed using specific transcutaneous oxygen sensors. The optimal location will depend on the commercial application. Criteria and restrictions will vary according to the use. These preliminary results are encouraging and demonstrate that our wearable device prototype has sufficient sensitivity to distinguish differences between measurement locations and also demonstrates the feasibility of collecting such data from human subjects in the lab setting.

REFERENCES

[1] *World Health Organization*: Coronavirus (COVID-19) Dashboard, [Online]. Available: https://covid19.who.int. [Accessed Jan.26, 2023].

[2] *World Health Organization*: The top 10 causes of death, [Online]. Available: https://www.who.int/news-room/fact-sheets/detail/the-top-10-causes-of-death. [Accessed Jan.26, 2023].

[3] D. Sen et al., "Contemporary and nascent techniques for monitoring of oxygenation as a vital sign," in *2020 IEEE 63rd International Midwest Symp. Circuits Syst (MWSCAS)*. IEEE, 2020, pp. 647–650.

[4] I. Costanzo et al., "A prototype towards a transcutaneous oxygen sensing wearable," in *IEEE Biomedical Circuits and Systems Conference (BioCAS)*, Oct. 2019, pp. 1–4.

[5] *Surveillance, Epidemiology and End Results (SEER) Program*: Physiology of Circulation, [Online]. Available: https://training.seer.cancer.gov/anatomy/cardiovascular/blood/physiology.html. [Accessed Jan.26, 2023].

[6] T. Rafferty et al., "Transcutaneous po2 as a trend indicator of arterial po2 in normal anesthetized adults," *Anesthesia & Analgesia*, vol. 61, no. 3, pp. 252–255, 1982.

[7] U. Guler, I. Costanzo, and D. Sen, "Emerging blood gas monitors: How they can help with covid-19," *IEEE Solid-State Circuits Magazine*, vol. 12, no. 4, pp. 33–47, 2020.

[8] I. Costanzo et al., "A noninvasive miniaturized transcutaneous oxygen monitor," *IEEE Transactions on Biomedical Circuits and Systems*, vol. 15, no. 3, pp. 474–485, Jun. 2021.

[9] S. A. Thy *et al.*, "Associations between clinical interventions and transcutaneous blood gas values in postoperative patients," *Journal of Clinical Monitoring and Computing*, pp. 1–10, 2023.

[10] I. Costanzo, D. Sen, and U. Guler, "An integrated readout circuit for a transcutaneous oxygen sensing wearable device," in *2020 IEEE Custom Integrated Circuits Conference (CICC)*. IEEE, 2020, pp. 1–4.

[11] B. Kahraman et al., "A miniaturized prototype for continuous non-invasive transcutaneous oxygen monitoring," *2022 IEEE Biomedical Circuits and Systems Conference (BioCAS)*, pp. 486–490, 2022.

[12] D. Blake et al., "Transcutaneous oximetry: variability in normal values for the upper and lower limb," *Diving and hyperbaric medicine*, vol. 48, no. 1, p. 2, 2018.

[13] A. Carreau et al., "Why is the partial oxygen pressure of human tissues a crucial parameter? small molecules and hypoxia," *Journal of cellular and molecular medicine*, vol. 15, no. 6, pp. 1239–1253, 2011.

[14] R. Samsel et al., "Oxygen delivery to tissues," *European Respiratory Journal*, vol. 4, no. 10, pp. 1258–1267, 1991.

[15] U. K. Franzeck et al., "Transcutaneous oxygen tension and capillary morphologic characteristics and density in patients with chronic venous incompetence." *Circulation*, vol. 70, no. 5, pp. 806–811, 1984.

[16] G. Basaranoglu et al., "Comparison of SpO_2 values from different fingers of the hands," *Springerplus*, vol. 4, no. 1, p. 561, 2015.

[17] *Keysight* E36103 A DC power supply, 20 V, 40 W 2 A: product datasheet, 2019. [Online]. Available: https://literature.cdn.keysight.com/litweb/pdf/5992-0914EN.pdf?id=2633187. [Accessed Dec.5, 2022].

[18] *Energizer* CR2032: product datasheet, [Online]. Available: https://data.energizer.com/pdfs/cr2032.pdf. [Accessed Dec.5, 2022].

[19] M. Quaranta *et al.*, "Indicators for optical oxygen sensors," *Bioanalytical Reviews*, vol. 4, no. 2-4, p. 115, Dec 2012.

[20] M. Y. Berezin and S. Achilefu, "Fluorescence Lifetime Measurements and Biological Imaging," *Chem. Rev.*, vol. 110, no. 5, p. 2641, May 2010.

[21] B. Kahraman et al., "Power and accuracy optimization for luminescent transcutaneous oxygen measurements," *2022 IEEE International Symposium on Circuits and Systems (ISCAS)*, pp. 1615–1619, 2022.

[22] *World Medical Association* Declaration of Helsinki: Ethical principles for medical research involving human subjects, [Online]. Available: https://www.wma.net/policies-post/wma-declaration-of-helsinki-ethical-principles-for-medical-research-involving-human-subjects/. [Accessed Dec.6, 2022].

[23] V. Vakhter *et al.*, "A prototype wearable device for noninvasive monitoring of transcutaneous oxygen," *IEEE Transactions on Biomedical Circuits and Systems*, 2023.

[24] "Cutaneous Carbon Dioxide (PcCO2) and Oxygen (PcO2) Monitors - Class II Special Controls Guidance Document for Industry and FDA," Dec. 2002. [Online]. Available: https://www.fda.gov/medical-devices/guidance-documents-medical-devices-and-radiation-emitting-products/cutaneous-carbon-dioxide-pcco2-and-oxygen-pco2-monitors-class-ii-special-controls-guidance-document